Journal of Computing and Electronic Information Management

ISSN: 2413-1660

One Image Restoration Method with a Combined Regularization

Xiaoguang Liu
School of Computer Science and Technology, Southwest University for Nationalities, Chengdu, Sichuan 610041, P. R. China
tianbian-235@163.com

Abstract: In the paper, we study a minimization method to restore the smooth images with neat boundaries. This method restores the images by using the GNC method based on combining Tikhonov and nonconvex nonsmooth regularizations. Finally, lots of numerical computation results are used to show the restored performance of the proposed method.

Keywords: smooth, neat boundary, Tikhonov, nonconvex nonsmooth, regularization, image restoration

1. Introduction

It is well known that one of the effective ways to deal with the image restoration is to define the regularization solution [1]. When the additive noise meets Gaussian distribution, the method of estimating the original image $\hat{f} \in R^p$ is to find a minimizer of the following energy function:

$$g = A\hat{f} + b, \tag{1}$$

where $p = p_1 \times p_2$ with p_1 and p_2 being the number of rows and columns respectively when image expressed as a matrix, $A \in R^{q \times p}$ represents the degradation system and $\boldsymbol{g} \in R^q$ is the observed image. The regularization term Φ embodies the priori information and $\alpha > 0$ is used to control the tradeoff.

In general, $\Phi(\boldsymbol{f}) = \sum_{i \in \mathrm{I}} \phi(t_i) = \sum_{i \in \mathrm{I}} \phi(\|D_i \boldsymbol{f}\|_2)$, $\mathrm{I} = \{1, 2, \cdots, p\}$ and $\phi : R \to R_+ = \{t \in R, t \geq 0\}$ is a potential function. $D_i \in R^{2 \times p}$ is used to construct the first order difference vector between the ith pixel and its two neighboring pixels. Here $D_i = [D_i^1; D_i^2]$ with

$\begin{cases} i \in \mathrm{I}_1 = \{p_2, 2p_2, \cdots, p_1 p_2\} \Rightarrow D_i^1[j] = 0, \forall j = 1, \cdots, p \\ i \notin \mathrm{I}_1 \Rightarrow D_i^1[i] = -1, D_i^1[i+1] = 1 \text{且} \forall j \notin \{i, i+1\}, \text{有} D_i^1[j] = 0 \end{cases}$, $\begin{cases} i \in \mathrm{I}_2 = \{(p_1 - 1)p_2 + 1, (p_1 - 1)p_2 + 2, \cdots, p_1 p_2\} \Rightarrow D_i^2[j] = 0, \ \forall j = 1, \cdots, p \\ i \notin \mathrm{I}_2 \Rightarrow D_i^2[i] = -1, D_i^2[i+p_2] = 1 \text{且} \forall j \notin \{i, i+p_2\}, \text{有} D_i^2[j] = 0 \end{cases}$.

As seen from [1–11], the potential function ϕ plays a important role in the image restoration. Tikhonov regularization $\Phi(\boldsymbol{f}) = \sum_{i \in \mathrm{I}} \|D_i \boldsymbol{f}\|_2^2$, i.e., $\phi(t_i) = t_i^2$ is widely used due to its differentiability and good restoration performance, but it tends to make images overly smooth and is only suitable to restore the smooth regions [2–4]. For the images with neat boundaries, nonconvex nonsmooth potential functions have reflected better restoration performance, which is proved in theory by M. Nikolova [5, 6]. However, the nonconvexity and nonsmoothness could cause many numerical computation difficulties such as the minimizer of energy function is not unique. Moreover, the excellent restoration performance of nonconvex nonsmooth regularizations could cause the staircase artifacts [7, 8], i.e., smooth transition regions in the intensity tend to be over-segmented to form some constant subregions

Based on the above considerations, one method based on combining Tikhonov and nonconvex nonsmooth regularizations is presented to restore the smooth images with neat boundaries in this paper. To avoid the numerical difficulties caused by the nonconvexity and nonsmoothness, the graduated nonconvexity (GNC) method [6, 8] will be employed. Finally, experimental results are provided to illustrate the effectiveness and efficiency.

2. Image restoration combining different regularizations

Let ϕ is nonconvex nonsmooth, then the energy function in (1) combining Tikhonov and the nonconvex nonsmooth regularizations is

$$J(f) = \|Af - g\|_2^2 + \sum_{i \in \mathrm{I}} (\alpha \phi(\|D_i f\|_2) + \gamma \|D_i f\|_2^2), \tag{2}$$

where α and γ are positive parameters. To get a good initial value of $\min\{J(f) \mid f \in R^p\}$, the GNC method adopts the following nonsmooth approximate energy functions to gradually approach $J(f)$:

$$J_{\varepsilon_k}(f) = \|Af - g\|_2^2 + \sum_{i \in \mathrm{I}} (\alpha \phi_{\varepsilon_k}(\|D_i f\|_2) + \gamma \|D_i f\|_2^2).$$

i.e., the minimizer of $J_{\varepsilon_{k-1}}(f)$ is set as the initial value of $\min\{J_{\varepsilon_k}(f) \mid f \in R^p\}$, where $0 = \varepsilon_0 < \varepsilon_1 < \cdots < \varepsilon_n = 1, \phi_{\varepsilon_n} = \phi$. As shown in [6], let $\phi_{\varepsilon_k}(t) = \varphi_{\varepsilon_k}(t) + \alpha_{\varepsilon_k} |t|$ and $\alpha_{\varepsilon_k} = \phi'_{\varepsilon_k}(0^+)$, then φ_{ε_k} is twice differentiable. Set $\psi_{\varepsilon_k}(\boldsymbol{f}) = \sum_{i \in \mathrm{I}} \varphi_{\varepsilon_k}(\|D_i \boldsymbol{f}\|_2)$, then we have

$$J_{\varepsilon_k}(f)=\|Af-g\|_2^2+\alpha\psi_{\varepsilon_k}(f)+\sum_{i\in \mathrm{I}}(\alpha\alpha_{\varepsilon_k}\|D_i f\|_2+\gamma\|D_i f\|_2^2) \tag{3}$$

Obviously, J_{ε_0} is convex nonsmooth, and J_{ε_k} is nonconvex nonsmooth for each $\varepsilon_k>0$. Thus some methods based on gradient such as Newton and CG could not be directly applied to solve the problem $\min\{J_{\varepsilon_k}(f)\mid f\in R^p\}$, and the following method is given accordingly.

Firstly, one auxiliary variable $u\in R^{2\times p}$ is used to cope with the nonsmooth term $\|D_i f\|_2$. The weighted quadratic fitting term $\omega\sum_{i\in \mathrm{I}}\|D_i f-u_i\|_2^2$ is added to ensure the closeness of $D_i f$ and $\boldsymbol{u}_i$, where ω is a positive parameter. Then the augmented form of (3) is

$$\hat{J}_{\varepsilon_k}(f,u)=\|Af-g\|_2^2+\alpha\psi_{\varepsilon_k}(f)+\sum_{i\in \mathrm{I}}(\alpha\alpha_{\varepsilon_k}\|u_i\|_2+\omega\|D_i f-u_i\|_2^2+\gamma\|D_i f\|_2^2).$$

Next, alternating direction method [9] is employed to find the minimizer of $\hat{J}_{\varepsilon_k}(f,u)$.

(i) f is fixed. The problem is

$$u^{(m,\varepsilon_k)}=\arg\min_u\sum_{i\in \mathrm{I}}(\alpha\alpha_{\varepsilon_k}\|u_i\|_2+\omega\|D_i f^{(m-1,\varepsilon_k)}-u_i\|_2^2),$$

which could be solved by the shrinkage algorithm [10], i.e.,

$$u_i^{(m,\varepsilon_k)}=\frac{D_i f^{(m-1,\varepsilon_k)}}{\|D_i f^{(m-1,\varepsilon_k)}\|_2}\max\left\{\|D_i f^{(m-1,\varepsilon_k)}\|_2-\frac{\alpha\alpha_{\varepsilon_k}}{2\omega},0\right\},\quad i\in \mathrm{I}.$$

(ii) u is fixed.

$$f^{(m,\varepsilon_k)}=\arg\min_f\|Af-g\|_2^2+\alpha\psi_{\varepsilon_k}(f)+\sum_{i\in \mathrm{I}}(\omega\|D_i f-u_i^{(m,\varepsilon_k)}\|_2^2+\gamma\|D_i f\|_2^2),$$

and it can be solved in the following two cases.

Case 1. $\varepsilon_k=0$. Now $\psi_{\varepsilon_k}(\boldsymbol{f})=0$, and the problem is equivalent to solving the system of the equations:

$$(A^{\mathrm{T}}A+\sum_{i\in \mathrm{I}}(\omega+\gamma)D_i^{\mathrm{T}}D_i)f^{(m,\varepsilon_k)}=A^{\mathrm{T}}g+\sum_{i\in \mathrm{I}}\omega D_i^{\mathrm{T}}u^{(m,\varepsilon_k)}.$$

Since $M=A^{\mathrm{T}}A+\sum_{i\in \mathrm{I}}(\omega+\gamma)D_i^{\mathrm{T}}D_i$ is positive definite, thus

$$f^{(m,\varepsilon_k)}=M^{-1}[A^{\mathrm{T}}g+\sum_{i\in \mathrm{I}}\omega D_i^{\mathrm{T}}u^{(m,\varepsilon_k)}].$$

Case *2.* $\varepsilon_k\neq 0$. The objective function is twice differentiable and nonconvex. Now, it needs to solve the system of the equations:

$$2M\Delta f^{(m-1,\varepsilon_k)}=-\nabla_{\mathrm{f}}\hat{J}_{\varepsilon_k},$$

where $\nabla_f \hat{J}_{\varepsilon_k}$ is the gradient about f , and the positive definite part $2M$ of the Hessian matrix is used to ensure that the search direction is a descent direction. Then let $\boldsymbol{f}^{(m,\varepsilon_k)} = \boldsymbol{f}^{(m-1,\varepsilon_k)} + \tau\Delta\boldsymbol{f}^{(m-1,\varepsilon_k)}$ with the step size $\tau > 0$.

In summary, the proposed algorithm can be described as follows :

Algorithm 1

Step 1. set ε_0=0 , $\Delta\varepsilon$=1/ n , $f^{(0,0)} = g$ and Abs = 10^{-4}(absolute error), initialize α, γ;

Step 2. if $\varepsilon_k + \Delta\varepsilon > \varepsilon_n$, then stop. Set $m = 1$ and ReErr=Abs+1(relative error), initialize ω ;

Step 3. compute $u^{(m,\varepsilon_k)}$, $f^{(m,\varepsilon_k)}$, and ReErr= $\left\| \boldsymbol{f}^{(m,\varepsilon_k)} - \boldsymbol{f}^{(m-1,\varepsilon_k)} \right\|_2 / \left\| \boldsymbol{f}^{(m,\varepsilon_k)} \right\|_2$;

Step 4. if ReErr > Abs, then increase ω, set $m = m + 1$ and goto step 3;

Step 5. set $f^{(0,\varepsilon_{k+1})} = f^{(m,\varepsilon_k)}$, $\varepsilon_{k+1} = \varepsilon_k + \Delta\varepsilon$,and goto step 2.

3. Experimental results

In this section, we will list the experimental results of algorithm 1 and two other classical image restoration algorithms in [4, 6], which the basic programmes are obtained from http://www.math.hkbu.edu.hk. Two tested images shown on Figures 1-2(a) are selected as Cameraman(CR) of 256 × 256, and jetplane(JP) of 512 × 512.

In all runs, CPU time is used to compare the efficiency. The quality of the restored images are measured by signal-to-noise ratio (SNR) and peak signal-to-noise ratio (PSNR) . The similarity between two images is evaluated by the structure similarity index measure (SSIM). As in [6], ω is initially set as 1.1, and it is updated by 1.8 times in each inner iteration, $\tau = 1$, $\phi(t) = \lambda|t| / (1 + \lambda|t|)$, $\phi_{\varepsilon_k}(t) = \lambda|t| / (1 + \varepsilon_k \lambda|t|)$ with $\lambda = 1$. The tested blurring function is truncated by 2-D Gaussian function:

$$h(s,t) = \exp\left(\frac{-s^2 - t^2}{2\sigma^2}\right)(-3 \le s, t \le 3),$$

where three sets of parameters are chosen: (1) σ = 0.5 and the support is 5×5; (2) σ = 1 and the support is 7 × 7; (3) σ = 1.5 and the support is 9 × 9, α = 0.015, γ = 0.03, n= 10. The standard deviation of Gaussian noise is set as 0.1 and 0.2. respectively.

As examples, let the standard deviation of noise is 0.1 and the support is 5 × 5, Figure 1(b)-(d) show the restored CR images by algorithms in [4], [6] and algorithm 1 respectively. Figure 2(b)-(d) show the restored JP images by algorithms in [4], [6], and algorithm 1 respectively, where the standard deviation of noise is 0.2 and the support is 9 × 9. We can observe from the two cases that the proposed method could not only

restore the smooth parts very well, but also preserve the neat boundaries in a better way. More restored results are summarized in Table 1-3.

With different noises and supports, Table 1-2 shows that the SNR, PSNR, and SSIM of the images restored by algorithm 1 are better than the results of the algorithms in [4, 6], which indicates that the proposed method could get better restored performance for smooth images with neat boundaries. It is a pity that Table 3 shows that algorithm1 has not obvious advantages in running time and ReErr(more similar results of other cases are omitted here).

(a) (b) (c) (d)

Fig. 1. The restored CR images by different algorithms with the standard deviation of noise is 0.1 and the support is 5×5. (a) Original image. (b) Image restored by algorithm in [4]. (c) Image restored by algorithm in [6]. (d) Image restored by algorithm 1

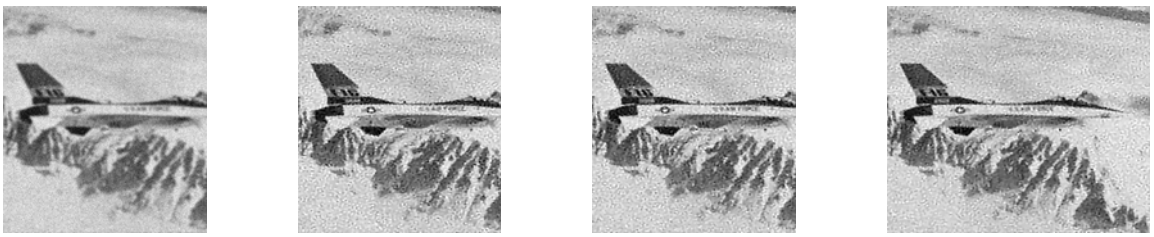

(a) (b) (c) (d)

Fig. 2. The restored JP images by different algorithms with the standard deviation of noise is 0.2 and the support is 9×9. (a) Original image. (b) Image restored by algorithm in [4]. (c) Image restored by algorithm in [6]. (d) Image restored by algorithm 1

Table 1 Restored results for CR image with different noises and blur levels

		SNR(db)			PSNR(db)			SSIM		
		[4]	[6]	OURS	[4]	[6]	OURS	[4]	[6]	OURS
0.1	5×5	20.74	20.72	20.88	25.33	25.37	25.56	0.9102	0.9074	0.9122
	7×7	19.32	19.30	19.46	25.40	25.39	25.61	0.9016	0.8979	0.9033
	9×9	17.82	17.87	18.01	23.54	23.57	23.65	0.8698	0.8687	0.8709
0.2	5×5	18.04	18.01	18.16	20.28	20.21	20.84	0.8307	0.8327	0.8336
	7×7	17.11	17.34	17.44	19.54	19.59	19.83	0.8230	0.8221	0.8237
	9×9	15.00	15.19	15.38	18.53	18.77	18.94	0.8212	0.8219	0.8219

Table 2 Restored results for JP image with different noises and blur levels

		SNR(db)			PSNR(db)			SSIM		
		[4]	[6]	OURS	[4]	[6]	OURS	[4]	[6]	OURS
0.1	5×5	21.11	21.31	21.48	24.39	24.34	25.01	0.8775	0.8763	0.8786
	7×7	20.84	20.65	20.87	22.31	22.42	22.51	0.8703	0.8709	0.8713
	9×9	17.98	17.99	18.13	20.51	20.54	20.71	0.8681	0.8687	0.8688
0.2	5×5	19.87	19.88	19.96	21.25	21.31	21.33	0.8734	0.8731	0.8736
	7×7	18.09	18.08	18.21	19.88	19.92	19.98	0.8701	0.8702	0.8712
	9×9	16.91	16.88	16.99	18.65	18.66	18.73	0.8648	0.8647	0.8649

Table 3 The running time and ReErr for different cases

		TIME(s)		
		[4]	[6]	OURS
0.1 (CR)	5×5	2.35	2.37	2.35
	7×7	2.91	2.90	2.92
	9×9	3.61	3.47	3.59
0.2 (JP)	5×5	6.05	6.13	6.22
	7×7	8.11	8.10	8.13
	9×9	9.71	9.77	9.62

4. Conclusion

Tikhonov regularization is usually restricted in the restoration of smooth images. Nonconvex nonsmooth regularization could bring some numerical computation difficulties and cause staircase artifacts, although it has good restoration performance

for the neat boundaries. With the aid of alternating optimization, the smooth images with neat boundaries are restored by the GNC method based on combining Tikhonov and nonconvex nonsmooth regularizations in this paper. The numerical results have illustrated that algorithm1 has better restored performance.

Acknowledgements

This work was supported in part by grant from the Fundamental Research Funds for the Central Universities of Southwest University for Nationalities 2015NZYQN30.

References

[1] R. C. Gonzalez, R. E. Woods, Digital Image Processing, 2nd ed., Prentice Hall Press, London, 2002.

[2] A. K. Katsaggelos, Digital Image Restoration, Springer-Verlag, 1991.

[3] D. C. Dobson and F. Santosa, Recovery of blocky images from noisy and blurred data, SIAM Journal on Applied Mathematics56(1996)1181-1198.

[4] Y. M. Wei, N. M. Zhang, M. K. Ng, W. Xu, Tikhonov regularization for weighted total least squares problems, Applied Mathematics Letters20(2007)82-87.

[5] M. J. Black, A. Rangarajan, On the unification of line processes, outlier rejection, and robust statistics with applications to early vision, International Journal of Computer Vision19(1996)57-91.

[6] M. Nikolova, M. K. Ng, C. P. Tam, Fast nonconvex nosmooth minimization methods for image restoration and reconstruction, IEEE Transation on Image Processing 19 (2010)3073-3088.

[7] W. Y. Sun, Y. X. Yuan, Optimization Theory and Method: Nonlinear Programming, Springer, 2006.

[8] L.Bedini, I.Gerace, A.Tonazzini, A GNC algorithm for constrained image reconstruction with continuous-value line process, Pattern Recognition Letters15 (1994)907-918.

[9] S. Boyd, N. Parikh, E. Chu, B. Peleato, J. Eckstein, Distributed optimization and statistical learning via the alternating directionMethod of multipliers, Foundations and Trends in Machine Learning3(2010)1-122.

[10] Y. Wang, J. Yang, W. Yin, Y. Zhang, A new alternating minimization algorithm for total variation image reconstruction, SIAM Journal Imaging Science1(2008)248-272.

[11] J. Yang, W. Yin, Y. Zhang, and Y. Wang, A fast algorithm for edge-preserving variational multichannel image restoration, SIAM Journal Imaging Science2(2009) 569-592.